Developmental Biology 340 (2010) 41–53

Contents lists available at ScienceDirect

Developmental Biology

journal homepage: www.elsevier.com/developmentalbiology

A mutation in the pericentrin gene causes abnormal interneuron migration to the olfactory bulb in mice

Setsu Endoh-Yamagami [a,b], Kameel M. Karkar [a,b,1], Scott R. May [b,2], Inma Cobos [c], Myo T. Thwin [c], Jason E. Long [c], Amir M. Ashique [a], Konstantinos Zarbalis [d], John L.R. Rubenstein [c], Andrew S. Peterson [a,*]

[a] Department of Molecular Biology, Genentech, Inc., South San Francisco, CA 94080, USA
[b] Department of Neurology, University of California San Francisco, San Francisco, CA 94158, USA
[c] Nina Ireland Laboratory of Developmental Neurobiology, Department of Psychiatry, University of California San Francisco, San Francisco, CA 94158, USA
[d] Department of Pathology and Laboratory Medicine, Davis Medical Center, University of California at Davis, Davis CA 95817, USA

ARTICLE INFO

Article history:
Received for publication 26 March 2009
Revised 8 January 2010
Accepted 14 January 2010
Available online 22 January 2010

Keywords:
Pericentrin
Interneuron migration
Brain development
Seckel syndrome
Microcephalic osteodysplastic primordial dwarfism (MOPD)
Schizophrenia
Rostral migratory stream (RMS)
Olfactory bulb

ABSTRACT

Precise control of neuronal migration is essential for proper function of the brain. Taking a forward genetic screen, we isolated a mutant mouse with defects in interneuron migration. By genetic mapping, we identified a frame shift mutation in the pericentrin (Pcnt) gene. The Pcnt gene encodes a large centrosomal coiled-coil protein that has been implicated in schizophrenia. Recently, frame shift and premature termination mutations in the pericentrin (PCNT) gene were identified in individuals with Seckel syndrome and microcephalic osteodysplastic primordial dwarfism (MOPD II), both of which are characterized by greatly reduced body and brain sizes. The mouse Pcnt mutant shares features with the human syndromes in its overall growth retardation and reduced brain size. We found that dorsal lateral ganglionic eminence (dLGE)-derived olfactory bulb interneurons are severely affected and distributed abnormally in the rostral forebrain in the mutant. Furthermore, mutant interneurons exhibit abnormal migration behavior and RNA interference knockdown of Pcnt impairs cell migration along the rostal migratory stream (RMS) into the olfactory bulb. These findings indicate that pericentrin is required for proper migration of olfactory bulb interneurons and provide a developmental basis for association of pericentrin function with interneuron defects in human schizophrenia.

Introduction

Proper function of the cerebral cortex requires appropriate migration and arrangement of neurons during development, and balanced networks among glutamatergic projection neurons and gamma-aminobutyric acid (GABA)-ergic interneurons. Projection neurons are generated in the ventricular zone (VZ) of the dorsal telencephalon, and they migrate radially toward the pial surface (Ayala et al., 2007; Marín and Rubenstein, 2003). On the other hand, interneurons are born in the subpallium, the ventral region of the telencephalon, and they migrate tangentially into the cortex or olfactory bulb (Ayala et al., 2007; Marín and Rubenstein, 2003; Wonders and Anderson, 2006). The subpallium can be divided into three major parts, the medial, lateral, and caudal ganglionic eminences (MGE, LGE, and CGE, respectively) (Flames et al., 2007). The CGE is largely the caudal extension of the dorsal LGE. While the MGE- and CGE-derived interneurons migrate mainly into the cortex, dorsal LGE (dLGE)-derived interneurons are thought to primarily migrate into the olfactory bulb along the rostral migratory stream (RMS). The neuronal migration along the RMS persists from embryonic stages into adulthood (Lois and Alvarez-Buylla, 1994). Although much progress has been made in understanding the mechanisms involved in radial migration of projection neurons, relatively little is known about the molecular and cellular mechanisms that regulate interneuron migration.

Previously, we performed a genetic screen to isolate mutant mice with defects in interneuron migration (Zarbalis et al., 2004). Analysis of one of the mutant mice led to the identification of a mutation in the pericentrin (Pcnt) gene. Pericentrin (also known as kendrin) is a large centrosomal coiled-coil protein with a PACT [pericentrin-AKAP450 (AKAP9) centrosomal targeting] domain in its C-terminus that targets it to the centrosome (Doxsey et al., 1994; Flory and Davis, 2003; Gillingham and Munro, 2000; Li et al., 2001). The centrosome is composed of a pair of centrioles surrounded by pericentriolar material (PCM). Pericentrin is localized to the PCM (Dictenberg et al., 1998), and it interacts with other centrosomal components including PCM1 and γ-tubulin ring complex proteins (Dictenberg et al., 1998; Li et al., 2001; Takahashi et al., 2002; Zimmerman et al., 2004). Diverse

* Corresponding author. Genentech, Inc. 1 DNA way, South San Francisco, CA 94080, USA. Fax: +1 650 225 6497.
E-mail address: peterson.andrew@gene.com (A.S. Peterson).
[1] Present address: Department of Neurology, University of Texas Health Science Center at San Antonio, San Antonio, TX 78229-3900, USA.
[2] Present address: Molecular Neurobiology Laboratory, The Salk Institute, La Jolla, CA 92037, USA.

0012-1606/$ – see front matter © 2010 Elsevier Inc. All rights reserved.
doi:10.1016/j.ydbio.2010.01.017

functions for this protein have been reported (for review, see Delaval and Doxsey, 2009), including microtuble nucleation and mitosis (Doxsey et al., 1994; Takahashi et al., 2002), cilia formation (Jurczyk et al., 2004; Martinez-Campos et al., 2004; Miyoshi et al., 2009), and as a centrosomal scaffold for multiple signaling proteins including protein kinase A (PKA) and protein kinase CβII (PKCβII) (Chen et al., 2004; Diviani et al., 2000). Pericentrin also interacts with Disrupted in Schizophrenia 1 (DISC1) and it has been implicated in schizophrenia (Matsuzaki and Tohyama, 2007; Miyoshi et al., 2004). Recently, single nucleotide polymorphisms (SNPs) in the human PCNT gene were reported to associate significantly with schizophrenia (Anitha et al., 2009), further supporting involvement of PCNT mutations in schizophrenia. Frame shift and premature termination mutations in the human PCNT gene have also been reported in Seckel syndrome (Griffith et al., 2008) and microcephalic osteodysplastic primordial dwarfism type II (MOPD II) (Rauch et al., 2008). Both diseases are characterized by proportional but severely reduced intrauterine and postnatal growth (primordial dwarfism) and microcephaly (defined as reduced head circumference more than 3 standard deviations below the normal mean for age, sex, race and gestation) often with mental retardation (Majewski and Goecke, 1982; Majewski and Goecke, 1998). These two diseases have been considered as two distinct disorders, but careful examination in recent studies demonstrated that Seckel syndrome individuals with PCNT mutations (PCNT-Seckel) show overlapping and comparable clinical features with MOPD II (Piane et al., 2009; Willems et al., 2009).

In this paper, we identified a mutation in the pericentrin gene through analysis of a perinatal lethal mutant mouse line that shows growth retardation and has a small brain with abnormal interneuron distribution and an olfactory bulb that is markedly reduced in volume. Further analysis indicated that dLGE-derived olfactory bulb interneurons are severely affected and distributed abnormally in the rostral forebrain in the mutant. We also found that knockdown of pericentrin expression impaired cell migration along the RMS into the olfactory bulb and that the mutant interneurons exhibited abnormal migration behavior. These findings demonstrate that pericentrin is essential for proper olfactory bulb interneuron migration and positioning.

Materials and methods

Mutation mapping and identification of a Pcnt mutant allele

Line 239 was isolated in a forward genetic screen as a mutant mouse line that shows abnormal interneuron distribution with the use of a Dlx-LacZ transgene (Zarbalis et al., 2004). In the screening strategy, male C57BL/6J mice were treated with ethyl-nitroso-urea (ENU) and then crossed to female FVB/NJ mice carrying the Dlx-LacZ transgene (Zarbalis et al., 2004). Unexpectedly, we found that the mutant phenotype of line 239 is linked to FVB/NJ markers on chromosome 10 and we concluded that line 239 carries a spontaneous mutation rather than an ENU-induced mutation. Outcrossing of line 239 to C57BL/6J was initiated, and meiotic recombination events/simple-sequence length polymorphism (SSLP) markers initially mapped the mutation between 10–76.57 (a marker generated in the Peterson lab; see Supplementary Table 1) and D10Mit42 (Mouse Genome Informatics, the Jackson laboratory; http://www.informatics.jax.org/) (see Supplementary Table 2). Fine scale mapping using 6 single nucleotide polymorphisms revealed that the line 239 mutation lies in a region between 74,610,791 and 76,175,591 on chromosome 10 in Mouse Ensembl release 48 (http://www.ensembl.org/Mus_musculus/index.html) harboring 40 genes and 1 pseudogene (Supplementary Table 2). Some of the genes did not appear to be expressed in E13.5 brain tissue and others were previously analyzed in knockout mice, and we did not sequence them (Supplementary Table 2). Sequencing all the exons of candidate genes revealed a mutation in the Pcnt gene.

Animal husbandry and genotyping

Heterozygous Pcnt ($Pcnt^{+/-}$, mutation on an FVB-derived chromosome) mice were maintained by crossing with C57BL/6. Outcrosses to C57BL/6 were performed at least 8 generations without changes in penetrance or variability of the mutant phenotype. The transgenic GAD67-GFP line (Tamamaki et al., 2003) was crossed to the $Pcnt^{+/-}$ line to generate $Pcnt^{+/-}$; GAD67-$GFP^{+/-}$ animals. The animals were crossed with the $Pcnt^{+/-}$ line to obtain $Pcnt^{-/-}$; GAD67-$GFP^{+/-}$ embryos. For slice electroporation, timed-pregnant FVB/N mice were purchased from Charles River Laboratories (Hollister, CA). Noon of the day of vaginal plug detection was termed as embryonic day (E) 0.5, and the day of birth as postnatal day (P) 0. All animals were handled in accordance with protocols approved by the Genentech Institutional Animal Care and Use Committee. Mouse colonies were maintained in a barrier facility at Genentech, conforming to California State legal and ethical standards of animal care. The Pcnt genotype was determined by PCR polymorphism or by sequencing (for primer information, see Supplementary Table 1). The $Pcnt^{-/-}$ embryos were also identified visually by polydactyly, a penetrant phenotype.

Histology

For immunofluorescent staining, mouse embryos or brains were fixed by immersion in 4% paraformaldehyde in phosphate-buffered saline and processed for paraffin sections at 10 μm. The antibodies used are as follows: mouse monoclonal anti-Pcnt (Pcnt mAb, 1:1000; BD Biosciences, San Jose, CA), rabbit anti-Pcnt (1:1000; Covance, Emeryville, CA), mouse monoclonal anti-γ-tubulin (γ-tubulin mAb, 1:1000; Sigma, St. Louis, MO), rabbit anti-γ-tubulin (1:1000, Sigma), anti-Ki67 (1:200, NeoMarkers, Fremont, CA), anti-βIII-tubulin (1:1000, Promega, Madison, WI), anti-PH3 (1:1000, Upstate, Temecula, CA), anti-cleaved caspase-3 (1:250, Cell Signaling Technology, Danvers, MA), anti-phospho-H2A.X (1:100, Cell Signaling Technology), anti-Pax6 (1:5, DSHB, Iowa, IA), anti-Tbr1 (1:1000, Millipore, Billerica, MA), anti-Nestin (1:1000, BD Biosciences) and fluorescent secondary antibodies (donkey anti-mouse, and anti-rabbit) conjugated with Alexa 488, 555 or 594 (1:400; Invitrogen, Carlsbad, CA). Images were acquired on a confocal microscope LSM 510 (Carl Zeiss, Thornwood, NY) and cell number counting was performed using ImageJ software (http://rsbweb.nih.gov/ij/).

In situ hybridization was performed on 20 μm frozen sections using digoxigenin-labeled riboprobes according to standard methods. The probes used and their sources are as follows: GAD67 (B. Condie); Dlx1 (generated in the Rubenstein lab); ER81 (T. Jessell); Tshz1 (X. Caubit); Lhx6 (V. Pachnis); Sst (T. Lufkin); Arx (K. Kitamura); ErbB4 (C. Lai); Pax6 (P. Gruss).

Immunoblot analysis

E14.5 brains were homogenized in RIPA buffer (20 mM Tris–HCl, pH 7.5, 150 mM NaCl, 1% NP-40, 0.5% sodium deoxycholate, 0.1% SDS, 1 mM EDTA, Complete protease inhibitor cocktail (Roche, Indianapolis, IN)). The same amount of protein was loaded in each lane, resolved by SDS-PAGE, transferred to PVDF membrane and detected with ECL-plus reagent (GE Healthcare, Piscataway, NJ) using Pcnt mAb (1:500; BD biosciences) or Pcnt Ab (1:1000; Covance).

DNA plasmid

To knockdown endogenous pericentrin protein expression, we used an miRNA-based vector system (Gray et al., 2007). A part of the CMV promoter of pShuttle-CMV/TO-miR (Gray et al., 2007) (kind gift

of D. Gray and D. Davis) was replaced by a chicken β-actin promoter to generate pChA_miR_EV using PCR primers described in Supplementary Table 1. miRNA hairpin sequences against the Pcnt gene were designed using the BLOCK-iT RNAi Designer (Invitrogen), and synthesized oligonucleotides (Supplementary Table 1) were annealed and inserted between the BsaI sites of pChA_miR_EV. For the negative control, a hairpin sequence described by Invitrogen was used. The target sequence is described in Supplementary Table 1.

Cell culture and dissociated cortical cultures

Murine inner medullary collecting duct (mIMCD-3) cells were obtained from ATCC (Manassas, VA) and maintained according to the ATCC instructions. Primary cortical cells were cultured on cortical feeders following the method of Xu et al.(Xu et al., 2004). Briefly, cortical cells were dissociated mechanically from the E16.5 wild-type or mutant cortex, and cultured in Neurobasl/B27 medium (Invitrogen) at a density of 2.5×10^5 cells/cm^2 as feeders 1 day before receiving donor cells. The dLGE of the rostral forebrain was microdissected from E13.5–E15.5 embryos, and dissociated cells were added at a low density to the feeders.

Slice electroporation and quantification of cell migration into the olfactory bulb

Preparation of slice cultures from the P1 mouse brain was carried out as previously described (Polleux and Ghosh, 2002). In brief, brains were embedded in 4% low-melting point agarose blocks and sagittally sectioned into 250 μm slices by vibratome (VT1000S; Leica). To achieve focal electroporation of RMS cells in the aSVZ, a DNA solution (1.5 μg/μl) with 0.005% Fast Green (Sigma) was injected through a glass micropipette into the RMS under the microscope. Electroporation was conducted as previously described with minor modifications (Stühmer et al., 2002). Four square wave pulses of 70 volts and 10 ms duration were applied using an ECM830 electroporator (BTX, Harvard Apparatus, Holliston, MA). Slices were maintained in organotypic slice cultures (Polleux and Ghosh, 2002), and inspected for proper targeting after 1 day in vitro (DIV) under epifluorescent dissection microscope. After 4 DIV, the slices were fixed and stained using Rabbit anti-GFP serum (1:2000; Invitrogen) as described (Polleux and Ghosh, 2002). Images were acquired on a LSM 510 confocal microscope. The GFP+ cells were counted in the olfactory bulb and RMS using Imaris software (Bitplane Inc., Saint Paul, MN), and the percentage of GFP+ cells in the olfactory bulb was calculated. By comparing with DAPI staining images, cells that were obviously transfected outside of the RMS were excluded and not counted.

Explant assay

Tissue pieces of the dLGE SVZ were microdissected from Gad67-GFP+ donor embryos (Pcnt$^{+/}$; GAD67-GFP$^{+/-}$ or Pcnt$^{-/-}$; GAD67-GFP$^{+/-}$ at E18.5) and explanted to the aSVZ of recipient sagittal brain slices (prepared from E18.5 Pcnt$^{+/}$ or Pcnt$^{-/-}$ embryos). Slices were cultured as described above, and the images were captured with M2 Bio fluorescence microscope (Carl Zeiss). At 3 DIV, proportion of GFP+ cells in the olfactory bulb was obtained. Since we confirmed that cell population ratio acquired by counting actual GFP+ cell number and by comparing GFP+ pixel number gives essentially the same results, we measured GFP+ pixel area in the olfactory bulb and RMS using MetaMorph analysis software (Molecular Devices, Sunnyvale, CA), and calculated the percentage of GFP+ cells in the olfactory bulb. To measure the migration speed, 1–2 DIV slices were monitored in real time by confocal LSM 510 inverted microscopy at 37 °C with 5% CO_2. Z-stacks of 19×4.45 μm optical sections were obtained every 11 min for 2–4.5 h. The obtained images were analyzed using Imaris software spot tracking function. The migration speed was compared between two groups using nested analysis of variance (ANOVA) using JMP software (v. 7.0; SAS Institute, Cary, NC).

Bromodeoxyuridine (BrdU) labeling assay

BrdU was administered by intraperitoneal injection (100 μl of 10 mg/ml BrdU solution per pregnant female mouse) at E14.5, and embryos were dissected and fixed at E17.5. Cells that incorporated BrdU were detected by anti-BrdU antibody (1:500, BD Biosciences). Cell distribution in the cerebral cortex was quantified as described previously (Hand et al., 2005).

Results

Identification of a Pcnt mutation in a dwarf mouse with abnormal interneuron distribution

Line 239 was isolated in a forward genetic screen to identify novel genes involved in interneuron migration with the use of a Dlx-LacZ transgene (Zarbalis et al., 2004). Animals homozygous for the line 239 mutation show aberrant aggregation of Dlx-LacZ positive cells in the rostral cortex and ectopic streaks of LacZ-expressing cells extending radially in the telencephalon (Zarbalis et al., 2004). To confirm the interneuron migration defects, we crossed the line 239 with the Gad67-GFP transgenic mouse line (Tamamaki et al., 2003). GAD67 (also known as Gad1) encodes an enzyme for GABA synthesis and marks GABAergic interneurons. In the wild-type or heterozygous mice, Gad67-GFP+ labels interneurons in the marginal zone (MZ) and subventricular zone (SVZ) of the cortex, and in the RMS and olfactory bulb (Fig. 1A). The homozygous mutant mice show abnormal ectopic streaks of GAD67-GFP+ interneurons extending radially from the anterior SVZ (aSVZ) in the rostral cortex (Fig. 1A). Homozygous mutant mice also display a progressive embryonic growth retardation and perinatal lethality (Figs. 1B, C). Mutants have a smaller brain than control littermates with a disproportionate reduction in the size of the olfactory bulbs (Figs. 1D, E, H, I). Growth retardation and microcephaly are well-known phenotypes observed in human syndromes with PCNT mutations, Seckel syndrome and MOPD II. Another characteristic feature of the line 239 is penetrant preaxial polydactyly (Zarbalis et al., 2004) (Figs. 1F, G).

To elucidate the underlying basis of the phenotype, we mapped the mutation to a specific chromosomal region and identified a two-nucleotide deletion mutation in exon 31 of the Pcnt gene (details in Materials and methods). The Pcnt gene encodes pericentrin, a large coiled-coil centrosomal protein (Doxsey et al., 1994; Flory and Davis, 2003; Li et al., 2001). At least three isoforms of pericentrin have been reported in mice (Flory and Davis, 2003; Miyoshi et al., 2006) (Fig. 1J). The frame shift mutation would disrupt all three isoforms, causing premature termination after 43 novel amino acids in Pcnt B and Pcnt S (Fig. 1J and Supplementary Fig. 1). The truncated proteins lack the C-terminal PACT domain that is involved in centrosomal targeting (Gillingham and Munro, 2000) (Supplementary Fig. 2). We had isolated two other mutant lines in the same screen, line 275 and line 251, with phenotypes that are very similar or identical to that of line 239 (Zarbalis et al., 2004). We found that line 275 has the identical causative Pcnt mutation as line 239 whereas the line 251 mutation maps to chromosome 7 and represents a distinct locus.

The frame shift mutation in Pcnt results in undetectable pericentrin at the centrosome

To examine how loss of the PACT domain affects centrosomal localization of pericentrin, we performed immunostaining with two different anti-pericentrin antibodies on brain sections of pericentrin mutant (Pcnt$^{-/-}$) and control littermates (Pcnt$^{+/}$) (Figs. 2A, B and Supplementary Fig. 3). In the Pcnt$^{+/}$ brain, pericentrin is highly

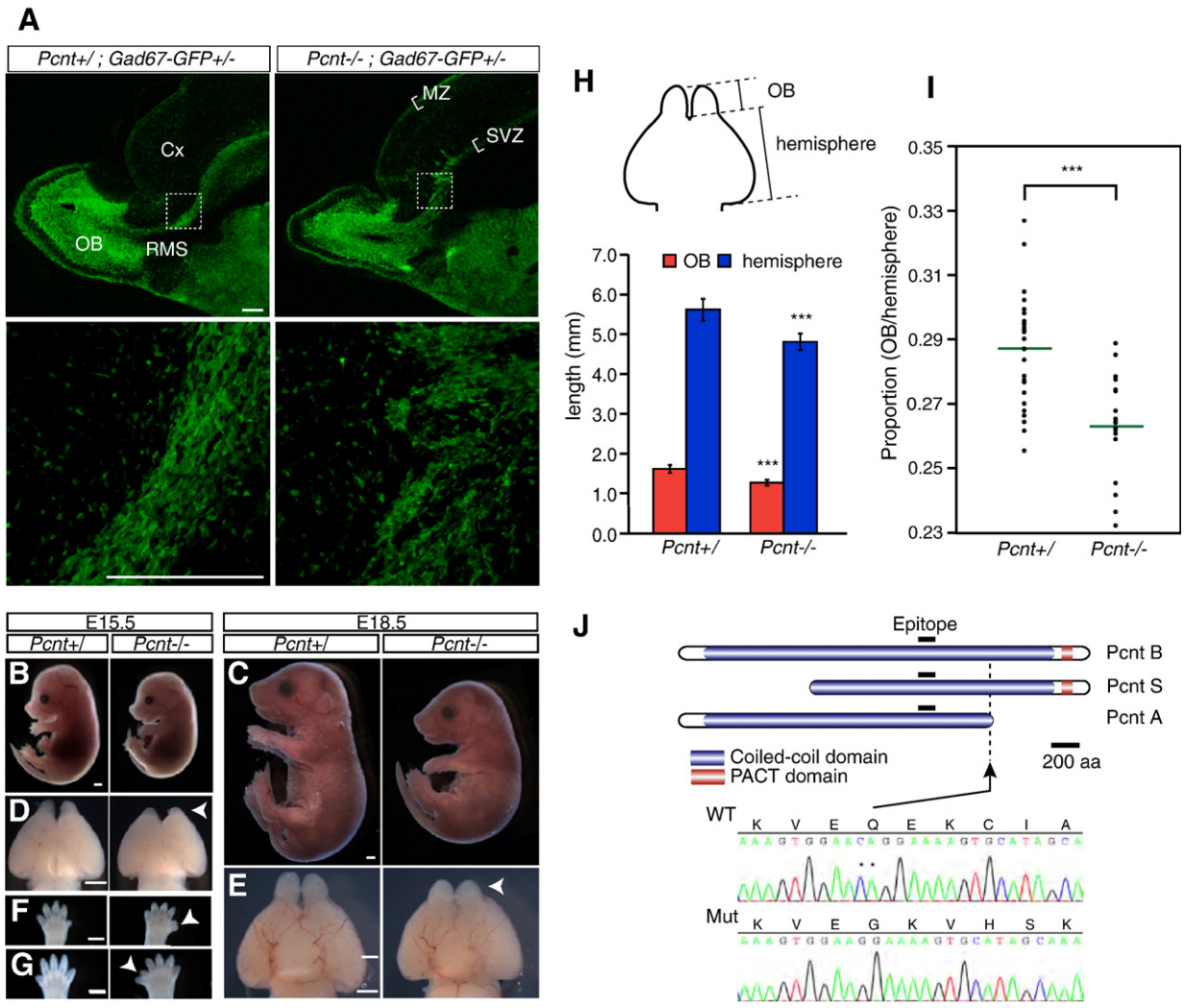

Fig. 1. Identification of a mutation in the *Pcnt* gene by analysis of the line 239 mutant. (A) Sagittal section of brains of E18.5 line 239 homozygous mutant ($Pcnt^{-/-}$) and control ($Pcnt^{+/}$) littermates. No differences in the phenotypes of wild-type and heterozygous ($Pcnt^{+/+}$ and $Pcnt^{+/-}$, respectively) embryos have been detected, and they were both used as controls ($Pcnt^{+/}$). Gad67-GFP shows abnormal positioning of interneurons in the cortex of the rostral telencephalon in the mutant. The Lower panels are close-up of the region shown by dotted line. OB, olfactory bulb; RMS, rostal migratory stream; Cx, cortex; MZ, marginal zone; SVZ, subventricular zone. Scale bars: 200 μm. (B, C) Gross appearance of E15.5 and E18.5 embryos. Line 239 homozygous mutant mice ($Pcnt^{-/-}$) show progressive growth retardation compared to control littermates. (D, E) Ventral view of the whole-mount telencephalon at E15.5 and E18.5. $Pcnt^{-/-}$ mice have smaller olfactory bulbs (arrowheads). (F, G) $Pcnt^{-/-}$ mice have penetrant anterior polydactyly (arrowheads). The E15.5 left forelimb (F) and right hindlimb (G) are shown. Scale bars: 1 mm (B–E). (H) Smaller olfactory bulbs and cerebral hemispheres in the mutant. The olfactory bulb and cerebral hemisphere length was measured as illustrated. The left and right sides were measured as replicates and the average value was calculated. The mean and standard deviation (SD) are graphed ($Pcnt^{+/}$, n = 29; $Pcnt^{-/-}$ n = 18 different animals). *** indicates $P < 0.0001$ (Student's t-test) (I) Disproportionally smaller olfactory bulbs in the mutant. The proportion of olfactory bulb to cerebral hemisphere length was calculated. Bars and *** indicate the mean values and $P < 0.0001$ (Wilcoxon test), respectively. (J) Schematic diagram of the pericentrin isoforms (Pcnt A, B, and S), and the mutation point in line 239. The 123 amino-acid epitope of mouse anti-Pcnt monoclonal antibody (Pcnt mAb; BD Biosciences) is indicated. An arrow indicates a mutation point in line 239. Sequence electrophoretograms depicting amino acid 2211–2219 in the wild-type (WT) and line 239 mutant (Mut) Pcnt gene. Line 239 mutant has a two-base pair deletion in exon 31 that results in a frame shift at codon 2214 of the Pcnt gene (GenBank/EBI/DDBJ accession number NM_008787.3 and Ensembl transcript ENSMUST00000001179). Asterisks indicate the nucleotides deleted in the mutant.

expressed in the ventricular zone (VZ), with polarized localization to the ventricular surface (Fig. 2A). Pericentrin staining has lower signal intensity in the SVZ/IZ, and a dispersed punctate staining pattern in the cortical plate (CP) (Fig. 2A). Consistent with these results, higher expression of Pcnt mRNA was observed in the VZ (Supplementary Fig. 3). Pericentrin is colocalized with the centrosomal protein γ-tubulin in the $Pcnt^{+/}$ brain, indicating centrosomal localization of pericentrin (Fig. 2B). However, centrosomal pericentrin staining was not detected in the mutant brain while the γ-tubulin staining pattern was not obviously different from that in the control brain (Fig. 2B).

Interneurons have readily apparent migratory defects in homozygotes (Zarbalis et al., 2004) (Fig. 1A). To examine pericentrin localization in the context of neuronal migration, we used expression of GAD67 to identify interneurons in dissociated cultures (Figs. 2C, D). The centrosome is located in the leading process of migrating interneurons (Métin et al., 2006) (Fig. 2D), and punctate localization of pericentrin is readily apparent in the leading process of wild-type interneurons (Fig. 2C). In the mutant interneurons, a γ-tubulin-positive centrosome is seen in the leading process (Fig. 2D), but centrosomal expression of pericentrin is not detectable (Fig. 2C).

By immunoblot analysis, we detected two major bands of about 330 kDa and 250 kDa in wild-type brain extract, corresponding to the molecular weight of pericentrin B and pericentrin A and/or S, respectively (Miyoshi et al., 2006) (Fig. 2E). The calculated molecular weight of the prematurely terminated mutant form of pericentrin is about 260 kDa, but no high molecular weight bands were recognized

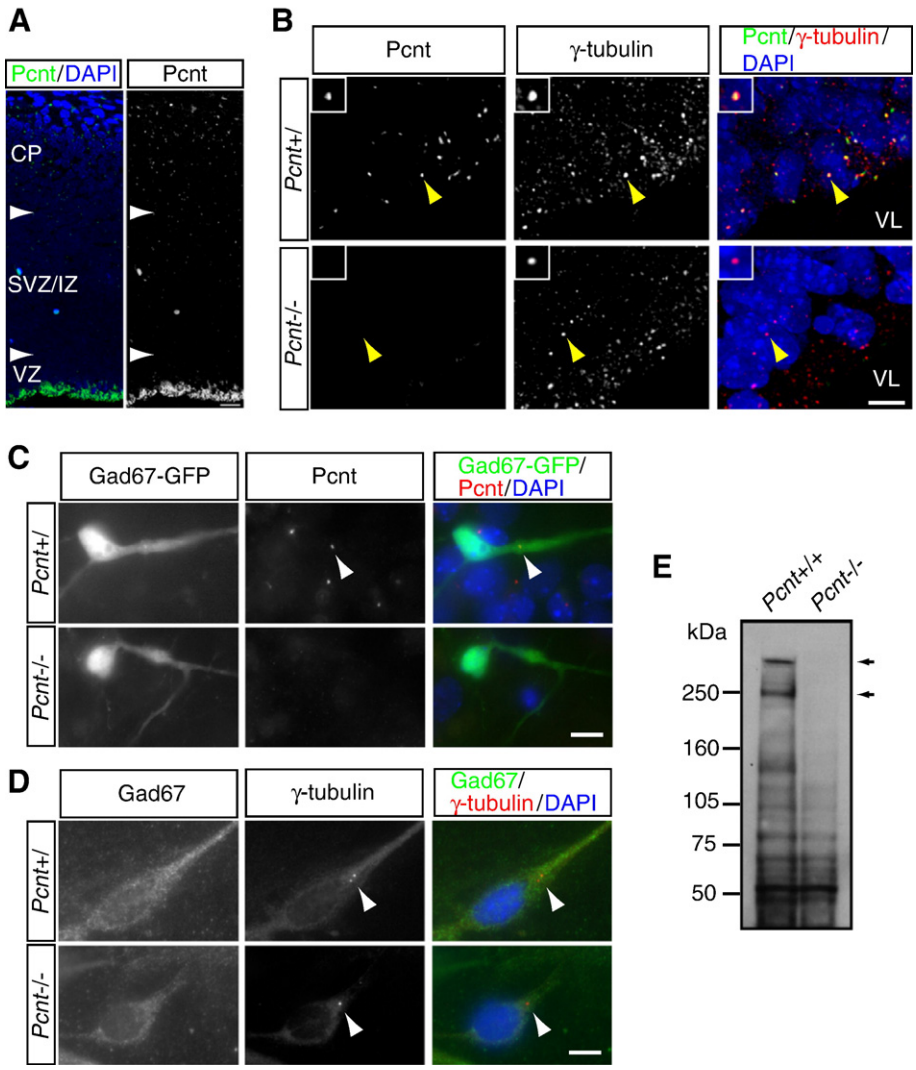

Fig. 2. Pericentrin localization is disrupted in the mutant. (A) Expression of Pcnt in E14.5 wild-type cerebral cortex. Mouse monoclonal Pcnt antibody raised against an epitope common to all three isoforms was used (see Fig. 1J). Strong signal of Pcnt-positive punctate staining is observed at the ventricular surface. Less prominent labeling of Pcnt-positive punctation is seen at the SVZ/IZ and CP of the cerebral cortex. Exposure, brightness and contrast were adjusted to show the low signal in the SVZ/IZ and CP. Scale bar: 20 μm. (B) Ventricular surface of the E14.5 brain. Confocal Z-stacks were obtained, deconvolved using Autoquant (version X2.0.1, Media Cybernetics) and projected. Pcnt (green) is localized to the centrosome in the $Pcnt^{+/}$ brain, indicated by γ-tubulin costaining (red). Centrosomal localization of Pcnt is not recognized in the $Pcnt^{-/-}$ brain. Inset is close-up of the centrosome indicated by arrowheads. VL, ventricular lumen. Scale bar: 5 μm. (C) Punctate localization of pericentrin is seen in the leading process of dorsal LGE (dLGE)-derived interneurons in the wild type (arrowhead), but not in the mutant. (D) A γ-tubulin-positive centrosome is seen in the leading process both in wild-type and mutant migrating dLGE interneurons (arrowheads). Scale bars: 10 μm (C,D). (E) Immunoblot of E14.5 brain extract with Pcnt mAb. Two major bands (arrows) are recognized at 330 kDa and 250 kDa in the wild-type brain, but they are absent in the $Pcnt^{-/-}$ brain.

in the mutant brain extracts (Fig. 2E), suggesting that the mutation destabilizes the protein and/or transcripts and further indicating that pericentrin function is largely abolished in the mutant.

The Pcnt mutation affects GAD67+ER81+Lhx6-interneurons

A characteristic feature of the line 239 phenotype is the pronounced defect in the rostral dispersion of interneurons visualized by Dlx-LacZ or Gad67-GFP (Zarbalis et al., 2004) (Fig. 1A). In the rostral cortex, aggregated Dlx-LacZ+ or Gad67-GFP+ cells (ectopias) are readily apparent whereas defects are not apparent in caudal areas of the cortex. To further characterize the interneuron phenotype, we performed in situ hybridization analysis for expression of several genes that mark migratory interneurons and their precursors on coronal sections of E15.5 and E18.5 control and mutant brains (Fig. 3 and Supplementary Fig. 4).

First, we examined expression of pan-GABAergic interneuron markers, GAD67 and Dlx1, in E15.5 brains. In the E15.5 control brain, GAD67 and Dlx1 showed a similar expression pattern, with expression in the olfactory bulb, septum and LGE of the rostral telencephalon, and LGE and MGE of the more caudal region (Figs. 3A–D and Supplementary Fig. 4). In the $Pcnt^{-/-}$ brain, GAD67 and Dlx1 showed reduced expression in the olfactory bulb, and ectopic radially-oriented stripes in the rostral dLGE and dorsal septum; this phenotype was not detectable in the caudal subpallium (Figs. 3A′–D′ and Supplementary Fig. 4). The rostral bias in the phenotype was consistent with the pattern of Dlx-LacZ and Gad67-GFP expression in mutants (Zarbalis et al., 2004) (Fig. 1A).

Next, we determined whether the ectopias were derived from specific subtypes of GABAergic interneurons, using expression of ER81, Tshz1, Lhx6 and Sst to distinguish between dLGE and MGE-derived interneurons (Figs. 3E–J′ and Supplementary Fig. 4). ER81 and Tshz1 are expressed in olfactory bulb interneurons and their progenitors in the dLGE (Caubit et al., 2005; Stenman et al., 2003) and perhaps the dorsal septum (Long et al., 2007). The Lhx6 gene is expressed in MGE and MGE-derived interneurons migrating into the

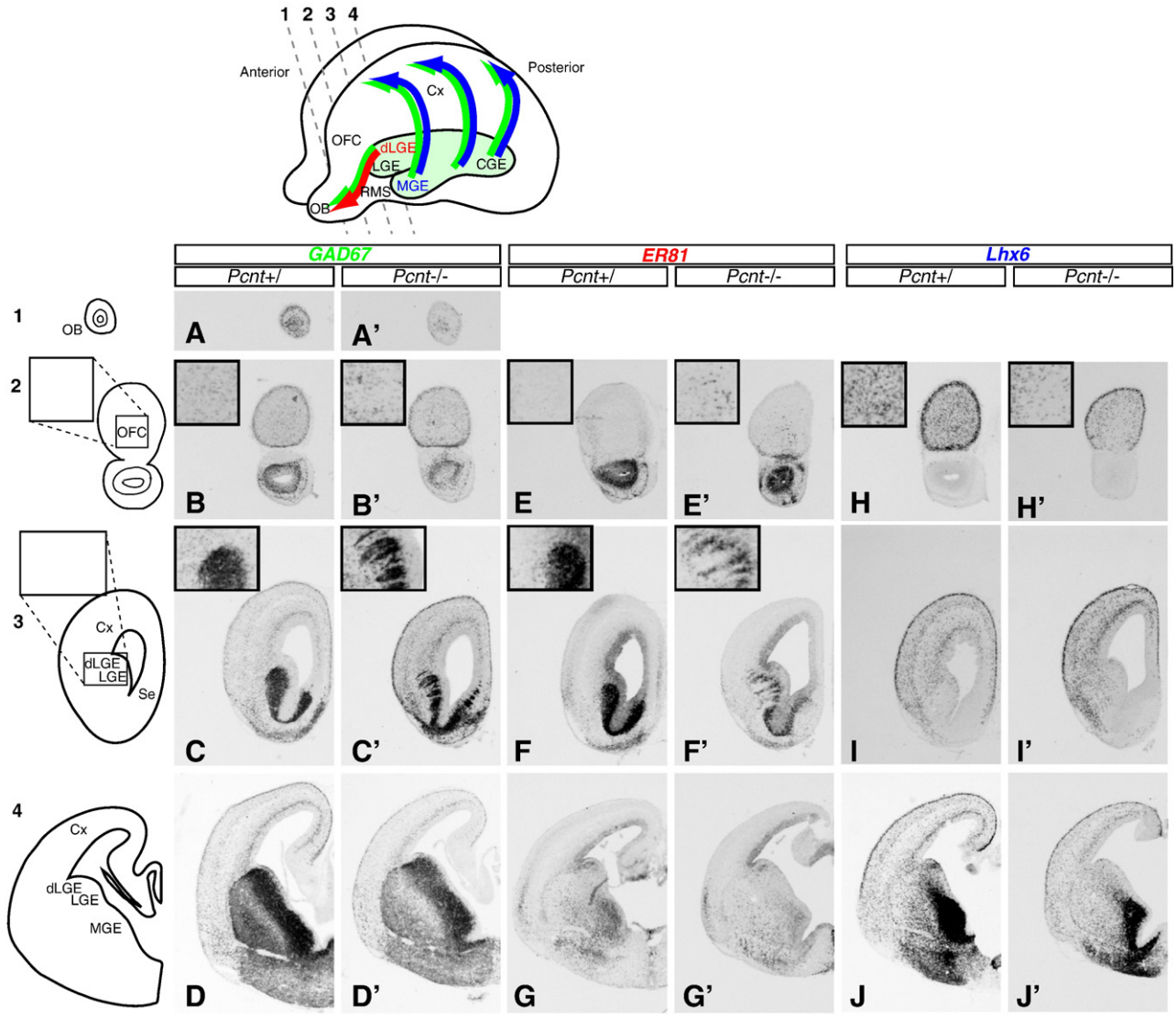

Fig. 3. Dorsal LGE-derived interneurons are affected in *Pcnt* mutant mice. In situ hybridization for interneuron markers in control and mutant brain at E15.5. Schematic illustration of interneuron migration pathways in the developing brain is shown. GAD67+ (green arrow) ER81+ (red arrow) interneurons migrate from the dLGE to the olfactory bulb along the RMS. GAD67+ (green arrow) Lhx6+ (blue arrow) interneurons migrate from the MGE to the cortex. Anterior to posterior (1 to 4) coronal sections were stained for pan-interneuron marker GAD67+ (A–D′), dLGE-derived interneuron marker ER81+ (E–G′), and MGE-derived interneuron marker Lhx6+ (H–J′). The insets show higher-magnification views of OFC (B,B′,E,E′,H,H′) and dLGE (C,C′,F,F′). OB, olfactory bulb; OFC, orbitofrontal cortex; Cx, cortex; Se, septum; LGE, lateral ganglionic eminence; dLGE, dorsal LGE; MGE, medial ganglionic eminence; CGE, caudal ganglionic eminence; RMS, rostral migratory stream.

cortex, and somatostatin+ (Sst+) interneurons in the cortex are also Lhx6+ (Liodis et al., 2007; Zhao et al., 2008). We found that Er81 (Fig. 3F′) and Tshz1 (Supplementary Fig. 4) showed ectopic radially-oriented stripes in the mutant's rostral dLGE and dorsal septum, whereas Lhx6 (Fig. 3I′) and Sst did not (Supplementary Fig. 4). In addition, Er81+ and Tshz1+ cells form ectopic punctate aggregates in the orbitofrontal cortex of the mutant, which were not observed in the control (Figs. 3E, E′ and Supplementary Fig. 4), while normally dispersed Lhx6+ and Sst+ cells were present in the orbitofrontal cortex of the mutant (Figs. 3H, H′ and Supplementary Fig. 4). These results support the idea that the ectopias are composed of dLGE- and/or dorsal septum-derived interneurons but not of MGE-derived interneurons. Analysis with additional markers, Arx, ErbB4 and Pax6 (Supplementary Fig. 4) supported this interpretation and further suggest that pericentrin is also necessary for proper positioning of dopaminergic interneurons as well as GABAergic interneurons in the olfactory bulb.

Pcnt is required for interneuron migration to the olfactory bulb cell-autonomously

Our finding that the Pcnt mutant has an abnormal distribution pattern of dLGE-derived interneurons and a reduced size of the olfactory bulb suggested that pericentrin is necessary for olfactory bulb interneuron progenitors to migrate properly into the olfactory bulb. To confirm this hypothesis, we performed a series of homotypic and heterotypic explants (Fig. 4). We microdissected a piece of tissue (donor) from the dLGE SVZ of E18.5 mutant or control mice carrying a GAD67-GFP gene, and explanted the donor tissue in the aSVZ of recipient brain slices. After culture for 3 days in vitro (DIV), the proportion of GFP+ cells that migrated into the olfactory bulb was determined (Fig. 4B). When GFP+ cells from $Pcnt^{+/}$ mice were explanted into either $Pcnt^{+/}$ or $Pcnt^{-/-}$ brain slices, comparable levels of cell migration to the olfactory bulb were observed (Figs. 4A, B). In contrast, when $Pcnt^{-/-}$ cells were explanted into either $Pcnt^{+/}$ or

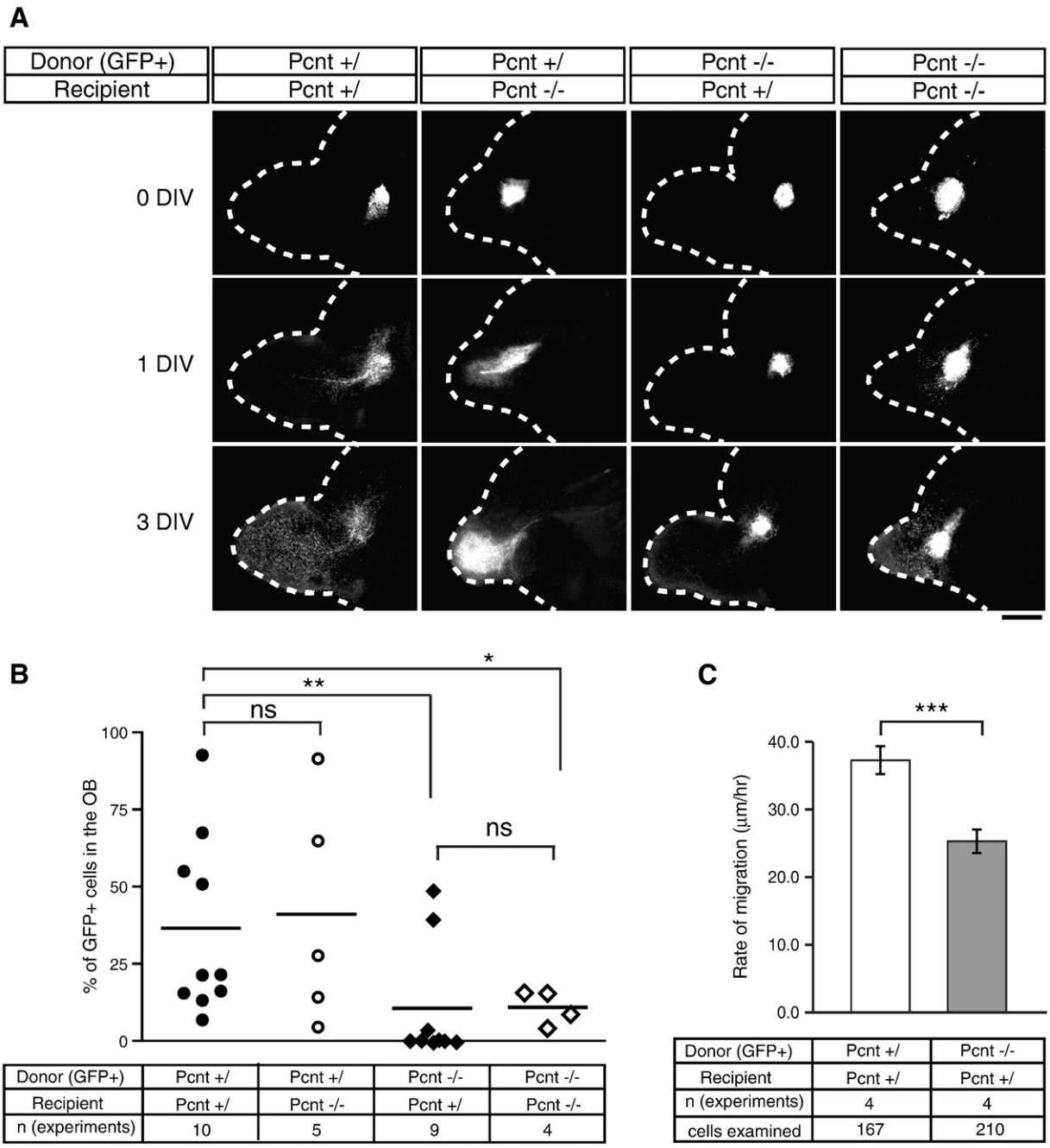

Fig. 4. Pcnt is required cell-autonomously for interneuron migration to the olfactory bulb. (A) Explant assay using different combinations of donors and recipients. Donor tissue pieces of the dLGE microdissected from Pcnt$^{+/}$; GAD67-GFP$^{+/-}$ or Pcnt$^{-/-}$; GAD67-GFP$^{+/-}$ E18.5 embryos were explanted to the aSVZ of recipient sagittal brain slices (E18.5 Pcnt$^{+/}$ or Pcnt$^{-/-}$). Brightness and contrast were adjusted using Adobe Photoshop (Adobe, San Jose, CA). Scale bar: 500 μm. (B) Proportion of cells that migrated into the olfactory bulb was determined at 3 DIV. Number of independent experiments using different animals is indicated. Bar: mean, *: $P<0.05$, **: $P<0.01$, ns: not significant (Wilcoxon test). (C) Slower migration rate of mutant interneurons in the RMS. Control or mutant GFP+ interneurons were explanted to Pcnt$^{+/}$ brain slices and monitored in real time by confocal microscopy between 1 and 2 DIV. Pcnt$^{-/-}$ interneurons migrated at a significantly slower rate (25.3 ± 1.7 μm/h, 4 independent experiments using different animals, 210 cells examined in total), compared to Pcnt$^{+/}$ interneurons (37.3 ± 2.1 μm/h, 4 independent experiments using different animals, 167 cells examined in total). Least Square Mean (LSM) and standard error of mean (SEM) are indicated. ***: $P<0.0001$ (nested analysis of variance (ANOVA)). See also Supplementary movies 1 and 2.

Pcnt$^{-/-}$ brain slices, a significant reduction in cell migration to the olfactory bulb was recognized compared to control homotypic explants (Pcnt$^{+/}$ on Pcnt$^{+/}$) (Figs. 4A, B). The genotypes of recipient animals did not contribute significantly in cell migration rate (Figs. 4A, B). These results demonstrate that pericentrin is required cell-autonomously for efficient interneuron migration to the olfactory bulb.

We further examined if the migration speed is affected by the pericentrin mutation (Fig. 4C and Supplementary movies 1 and 2). Control or mutant Gad67-GFP+ cells were explanted into control brain slices and allowed to migrate into the RMS. Between 1–2 DIV, migrating GFP+ interneurons were monitored in real time by confocal microscopy. While Pcnt$^{+/}$ interneurons migrated at a rate of 37.3 ± 2.1 μm/h (least square mean ± SEM, 4 independent experiments using different animals, 167 cells examined in total), Pcnt$^{-/-}$ interneurons migrated at a significantly slower rate (25.3 ± 1.7 μm/h, 4 independent experiments using different animals, 210 cells examined in total, $P<0.0001$ nested ANOVA). These results indicate that the pericentrin mutation impairs the net rate of interneuron migration in the RMS.

We also examined interneuron migration behavior in acute brain slices prepared from E13.5 Pcnt$^{+/+}$; GAD67-GFP$^{+/-}$ and Pcnt$^{-/-}$;

GAD67-GFP$^{+/-}$ embryos (Supplementary Fig. 5, and Movies 3 and 4). Focusing on migration of individual interneurons, we evaluated various parameters of migratory behavior of wild-type and mutant Gad67-GFP+ cells located in the rostral ventral forebrain where interneurons are abnormally distributed. In wild-type brain slices, we observed the characteristic behaviors of migrating interneurons including saltatory somal translocation and pauses (Métin et al., 2006) (Supplementary Fig. 5). The mutant Gad67-GFP+ interneurons on average showed a decreased net rate of migration, shorter somal translocations, fewer translocations per hour, longer pauses, and fewer direction changes (Supplementary Fig. 5). These results indicate that mutant interneurons also show abnormal migration behavior at earlier stages of development.

Pcnt knockdown reduces interneuron migration along the RMS to the olfactory bulb

To further confirm that pericentrin function is required for interneuron migration to the olfactory bulb, we asked whether pericentrin knockdown affects interneuron migration in the RMS. An miRNA-based Pcnt-knockdown plasmid (Figs. 5A, B) was injected into the RMS and introduced into cells by electroporation (Figs. 5C, D). Cell migration in the RMS was observed during in vitro slice culture (Fig. 5E). Cells expressing Pcnt-knockdown plasmid showed a significant decrease in migration into the olfactory bulb, compared to the negative control (Figs. 5F, G). Likewise, decreased cell migration was observed when a GFP-expressing plasmid was electroporated in Pcnt$^{-/-}$ brain slices compared to the control (Supplementary Fig. 6). These results further support our conclusion that pericentrin plays an important role in interneuron migration in the RMS to the olfactory bulb and that the effects of pericentrin loss are cell autonomous.

Cerebral cortex phenotype in the Pcnt mutant

To investigate whether the Pcnt mutation affects the structure of the cerebral cortex, we examined Pax6 and Tbr1, and nestin expression in the dorsal cerebral cortex of E14.5 mice (Fig. 6A). Pax6 is expressed in the VZ by cortical radial glia cells (Götz et al., 1998), and Tbr1 is expressed strongly in the subplate (SP), cortical plate and marginal zone, and weakly in the IZ by postmitotic projection neurons (Hevner et al., 2001). Although the cortex is thinner in the mutant, no obvious defects in cortical lamination are recognizable from Pax6 and Tbr1 staining (Fig. 6A). Radial glia that can be visualized by nestin antibody serves as a scaffold for neuronal migration and also as embryonic neural progenitors. Radial glia structures in the mutant did not show obvious defects in the mutant (Fig. 6A). Nissl staining of the cerebral cortex at the later stage, E18.5, also did not show prominent abnormality (Fig. 6B). More subtle defects, however, are possible.

To look more closely, we labeled cells by BrdU at E14.5 and examined their distribution at E17.5 (Figs. 6C, D). In the developing cerebral cortex, neuronal progenitors are mitotic active at the ventricular zone, and they incorporate BrdU and migrate radially to the pial surface. Unexpectedly, we found that the mutant shows different distribution pattern of BrdU-positive cells from the control mice. The Pcnt mutant has less BrdU+ cells at the ventricular surface and increased cells at the cortical plate (Fig. 6D). These results suggest that the pericentrin mutation affects radially migrating neurons as well as rostrally migrating interneurons, although the effects appear to be different between them. In contrast to the defective and decreased migration of olfactory bulb interneurons, the radial migration seems to occur.

To analyze whether the Pcnt mutation leads to changes in cell proliferation, we looked at expression of Ki67, an active cell cycle marker, and Phospho-histone H3 (PH3), a mitosis marker in the E14.5 control and mutant brains (Fig. 6E). Ki-67 positive proliferating cells and the βIII-tubulin-positive postmitotic neurons are recognized in the VZ/SVZ/IZ and CP, respectively, both in the control and mutant cortices (Fig. 6E). PH3 expression is seen in cells at the ventricular surface and transiently amplifying progenitors in the SVZ/IZ (Fig. 6E), and no obvious difference in cell proliferation is observed between control and mutant brains. We then asked whether the Pcnt mutation induces apoptosis. Cleaved caspase-3 expression revealed increased apoptosis in the Pcnt mutant (Fig. 6E). We also found increased expression of γ-H2A.X (histone H2A.X phosphorylated on serine 139), a marker for DNA double-strand breaks, in the mutant, which suggests increased DNA double-strand breaks in the Pcnt mutant. It can be inferred that increased DNA damages lead to more apoptosis in the mutant. We found that apoptosis was increased throughout the brain and body of the mutant (Supplementary Fig. 7). Apoptotic cells were uniformly distributed throughout the brain and there was no indication of a rostrally sensitive population (Supplementary Fig. 7). Thus, increased apoptosis does not seem to correlate with interneuron phenotype of the Pcnt mutant but it could be a contributor to dwarfism.

Discussion

We have identified a mutation in the *Pcnt* gene that underlies abnormal interneuron distribution in the rostral telencephalon of mice, and have demonstrated the involvement of pericentrin in brain development. The pericentrin mutation affects interneuron migratory behavior cell-autonomously and disrupts proper distribution of dLGE-derived olfactory bulb interneurons. Pericentrin is a large protein, and multiple functions of this protein can be inferred from its interaction with several other proteins, including centrosomal proteins and signaling proteins (Chen et al., 2004; Delaval and Doxsey, 2009; Dictenberg et al., 1998; Diviani et al., 2000; Li et al., 2001; Takahashi et al., 2002; Zimmerman et al., 2004). Future studies will address the question of why dLGE-derived interneurons are strongly affected by the pericentrin mutation. Our findings indicate an important role of pericentrin in the developing brain, and may have implications for its involvement in diseases of the cenrtral nervous system (CNS) that are closely linked to defects during development.

Pcnt and the etiology of psychiatric disorders

The role of pericentrin in interneuron development is of special interest with respect to the etiology of psychiatric disorders, such as schizophrenia and bipolar disorder. Schizophrenia is reported to be accompanied by reduced olfactory bulb volume (Turetsky et al., 2000) and by dysfunction of the prefrontal cortex that may be related to alterations in GABA neurotransmission (Lewis et al., 1999). The pericenterin mutant mice show small olfactory bulbs and GABAergic interneuron abnormalities in the prefrontal cortex. Pericentrin is known to interact with DISC1 and PCM1 (Li et al., 2001; Miyoshi et al., 2004). *DISC1* and *PCM1* are susceptibility genes for schizophrenia (Gurling et al., 2006; Jaaro-Peled et al., 2009; Matsuzaki and Tohyama, 2007). Indeed, significant association of *PCNT* SNPs with schizophrenia in the Japanese population was reported recently (Anitha et al., 2009). More recently, an independent group reported that they did not find any significant association of *PCNT* SNPs with schizophrenia in the Japanese population (Numata et al., 2009b), and studies in other populations are awaited to further clarify the linkage between *PCNT* and schizophrenia. The same group, on the other hand, reported positive association between the *PCNT* SNPs and major depressive disorder (Numata et al., 2009a). In addition, the human *PCNT* gene is located on chromosome 21q22.3, a locus that multiple linkage studies have correlated with bipolar disorder (Baron, 2002). Enhanced expression of *PCNT* was also reported in a Japanese population of bipolar disorder patients (Anitha et al., 2008). These studies highlight the potential involvement of the *PCNT* gene in psychiatric disorders. Interestingly, all *PCNT* mutations identified in PCNT-Seckel and MOPD

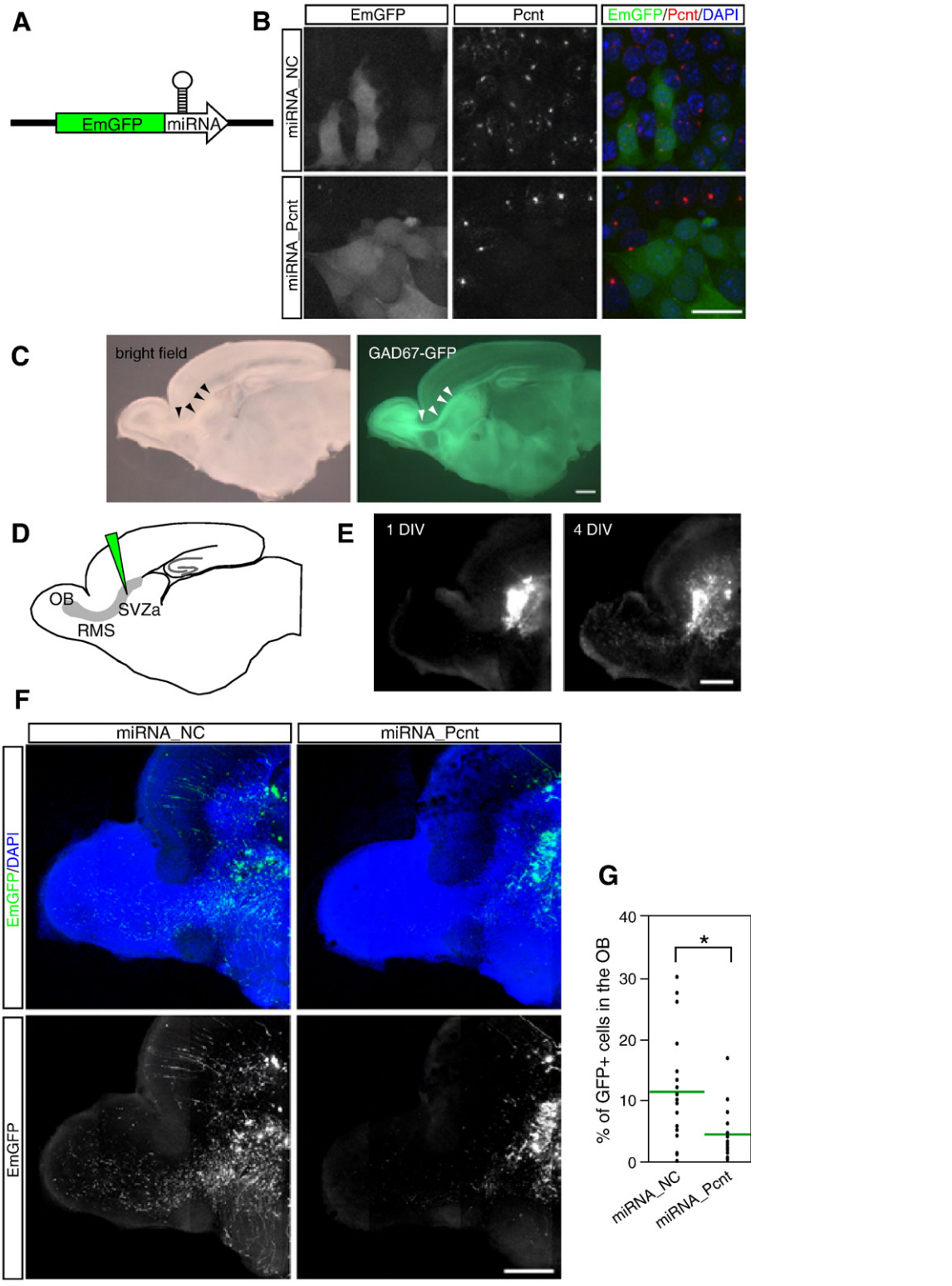

Fig. 5. Knockdown of pericentrin impairs interneuron migration along the RMS. (A) A schematic diagram of the miRNA construct. A plasmid was transfected to express an siRNA sequence embedded in an miRNA environment placed downstream of the EmGFP (emerald Green Fluorescent Protein) gene. (B) miRNA against Pcnt efficiently knocks down the endogenous Pcnt expression. mIMCD-3 cells were transfected with miRNA that targets all three of the known pericentrin isoforms (miRNA_PCNT) or negative control (miRNA_NC), and fixed 72 h after transfection. Pcnt expression is not recognized in miRNA_PCNT expressing cells (EmGFP-positive cells), while it is not affected in miRNA_NC expressing cells. Scale bar: 20 μm. (C) The RMS can be recognized as a dense cell population under the bright-field microscopy (black arrowheads) in P1 sagittal brain slices, verified by a correspondence to the GAD67-GFP positive stream (white arrowheads). (D) Experimental assay used to examine Pcnt-knockdown effect on neuron migration along the RMS. A DNA solution was injected into the RMS in anterior SVZ (aSVZ) and introduced into cells by electroporation. (E) Example of focal electroporation in the organotypic cultures of P1 brain slices, showing migration of cells electroporated with a plasmid expressing fluorescent protein. The same slice was photographed after 1 and 4 day in vitro (DIV). (F) Representative pictures of P1 brain slices that were electroporated with negative control or Pcnt-knockdown miRNA plasmid, fixed after 4 DIV and stained by GFP antibody. (G) Quantification of percentage of GFP+ cells in the olfactory bulb (GFP+ cells in the OB/cells in the RMS plus OB) after 4 DIV shows that a significant decrease in cell migration into the olfactory bulb is produced by Pcnt knockdown. Bars indicate the mean values: miRNA_NC; 11.27 (n = 18 different slices, 5567 cells counted in total), miRNA_Pcnt; 4.32 (n = 15 different slices, 4924 cells counted in total). *: $P < 0.05$ (Wilcoxon test). Scale bars: 500 μm (C, E, F).

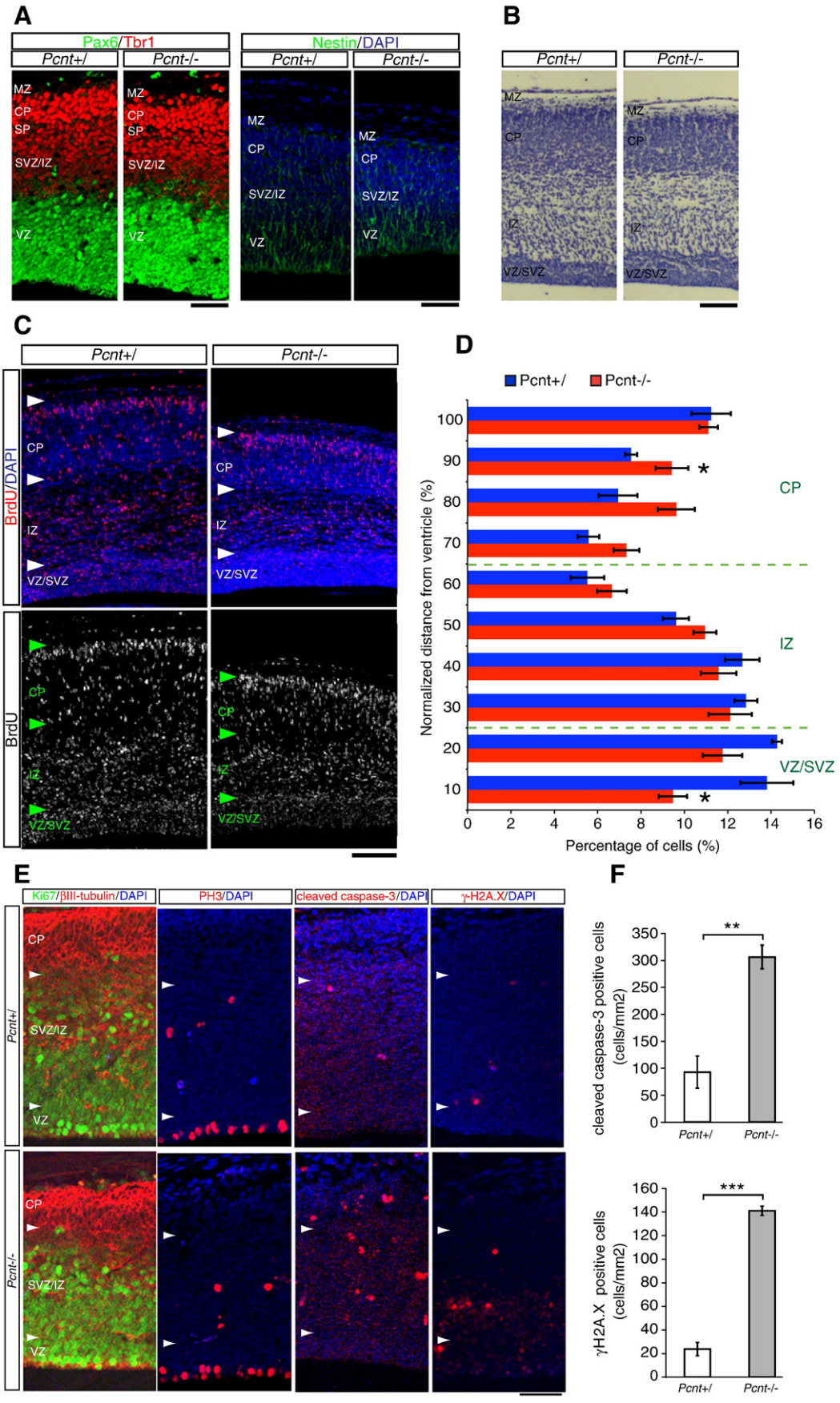
A
Pax6/Tbr1
Nestin/DAPI
Pcnt+/
Pcnt-/-
MZ
CP
SP
SVZ/IZ
VZ
B
IZ
VZ/SVZ
C
BrdU/DAPI
BrdU
D
Pcnt+/
Pcnt-/-
Normalized distance from ventricle (%)
Percentage of cells (%)
E
Ki67/βIII-tubulin/DAPI
PH3/DAPI
cleaved caspase-3/DAPI
γ-H2A.X/DAPI
F
cleaved caspase-3 positive cells (cells/mm2)
γH2A.X positive cells (cells/mm2)

II are nonsense, frame shift, or splicing mutations (Griffith et al., 2008; Piane et al., 2009; Rauch et al., 2008; Willems et al., 2009), and altered expression or missense milder mutations might be expected in psychiatric disorders. Thus, studying the role of pericentrin in brain development is expected to make a contribution in the field of mental disorders.

It is also noteworthy that olfactory bulb interneuron migration along the RMS is defective in mice deficient in ErbB4, another schizophrenia susceptibility factor (Anton et al., 2004; Jaaro-Peled et al., 2009). Future studies should address whether or not other schizophrenia susceptibility factors, including DISC1 and PCM1, are also required for olfactory bulb interneuron migration.

Seckel syndrome and CNS anomalies

Central nervous system (CNS) abnormalities are known in Seckel syndrome with microcephaly, mental retardation and seizures. CNS anomalies have been described in this syndrome, including agenesis of the corpus callosum, hypoplasia of cerebellar vermis, pachygyria, a dorsal cerebral cyst, gyral hypoplasia, macrogyria, and semilobar holoprosencephaly (Capovilla et al., 2001; Kumar et al., 2008; Shanske et al., 1997). Shanske et al. suggested that neuronal migration abnormalities may exist commonly in Seckel syndrome individuals and that Seckel syndrome should be included with other neuronal migration disorders (Shanske et al., 1997). However, CNS malformation is not always clear and further imaging studies are required to clarify the true incidence of CNS anomalies in Seckel syndrome (Carfagnini et al., 1999). Our report describes abnormal interneuron migration in the *Pcnt* mutant mice and suggests that interneuron distribution might also be affected in PCNT-Seckel individuals.

Centrosome and neuronal migration

The centrosome is known to serve as the microtubule-organizing center (MTOC) during mitosis, but other important functions for this organelle are being uncovered, including its role in neuronal migration (Badano et al., 2005; Higginbotham and Gleeson, 2007). Reflecting its various cellular functions, centrosomal proteins are involved in a wide variety of human genetic diseases (Badano et al., 2005). Dysfunction of centrosome-associated cytoskeletal components, such as the lissencephaly-1 (LIS1) and doublecortin (DCX), causes neuronal migration defects and results in lissencephaly (smooth brain) (Badano et al., 2005; Higginbotham and Gleeson, 2007; Tsai and Gleeson, 2005). In migrating neurons, including olfactory bulb interneurons migrating along the RMS, the centrosome is located in the leading process in front of the nucleus in the direction of migration (Bellion et al., 2005; Higginbotham et al., 2006; Solecki et al., 2004), which is considered as an important step of neuronal migration (Badano et al., 2005; Higginbotham and Gleeson, 2007; Tsai and Gleeson, 2005).

The γ-tubulin-positive centrosome was recognized in the leading process of dLGE-derived migrating interneurons in the *Pcnt* mutant as well as in the wild type (Fig. 2D), suggesting that centrosomal positioning is not affected. However, the absence of pericentrin, a component of the centrosome, means that the centrosome is not intact in the mutant. The centrosomal dysfunction might cause the olfactory bulb interneuron migration defects.

Phenotype in the cerebral cortex

While abnormal migration and distribution of olfactory bulb interneurons was found as one of the most striking brain phenotypes in the *Pcnt* mutant, other subtle defects are possible. Cells that incorporated BrdU at E14.5 showed a different distribution pattern in the cerebral cortex between control and mutant mice at E17.5 (Figs. 6C, D). Although we cannot distinguish cells that might have migrated from places other than the VZ of the cortex, the majority of BrdU+ cells in the cortex are considered to arrive via centrifugal radial migration. The distribution pattern of BrdU+ cells in the mutant, fewer cells at the ventricular surface and increased cells at the cortical plate, is reminiscent of DISC1 knockdown experiments performed by Mao et al. recently (Mao et al., 2009). Electroporation of DISC1 knockdown constructs with GFP-expressing vector into E13 embryos results in reduction of GFP+ cells in the ventricular zone and a corresponding increase in cells in the cortical plate at E15, which is explained by increased cell cycle exit and premature neuronal differentiation by DISC1 knockdown (Mao et al., 2009). It is plausible, considering physical interaction between Pcnt and DISC1 (Miyoshi et al., 2004), that the *Pcnt* mutant shows a similar pattern due to the same mechanism.

Increased apoptosis and DNA damage checkpoint signaling

It was recently reported that Seckel syndrome individuals with PCNT mutations (PCNT-Seckel) have defects in ATR-dependent cell cycle checkpoint and that lymphoblastoid cell lines established from PCNT-Seckel individuals are defective in the G2/M checkpoint response to UV-induced DNA damage (Griffith et al., 2008). Mouse embryonic fibroblasts established from the Pcnt mutant, however, did not show defects in G2/M checkpoint activated by UV-induced DNA damages (our unpublished data). We do, however, observe increased DNA double-strand breaks in the Pcnt mutant brain (Figs. 6E, F). Since the ATR-signaling pathway plays a major role in the S-phase checkpoint, which responds to DNA lesions that are generated during normal DNA replication, Pcnt mutant mice might accumulate DNA damage due to defects in the S-phase checkpoint and result in increased apoptosis. We are actively investigating this aspect of the Pcnt mutant phenotype, but we have not found any relationship between the increased rate of DNA double-strand breaks and interneuron migration defects, and these appear to be unrelated phenotypes. It is not surprising that the pericentrin mutation produces phenotypes that result from effects on different cellular functions, given that pericentrin is a multifunctional large protein binding to various factors (Delaval and Doxsey, 2009).

Acknowledgments

We thank F. Polleux and D. Bortone for sharing plasmids, techniques of electroporation and slice culture, and a method for cell migration quantification. We also thank Y. Choe for his technical help in Pcnt immunoblot analysis. We thank D. Gray and D. Davis for the miRNA vector plasmid and advice, J. Starks, M. Nee and R. Asuncion and C. Byers for animal husbandry, I. Fodor, M. Friesenhahn, A. Hartford, W. Forrest and N. Lewin-Koh for advice in statistics, and M. Solloway, D. Slaga and A. Minn for careful reading of this manuscript. The Pax6 antibody developed by A. Kawakami was obtained from the Developmental

Fig. 6. Analysis of cerebral cortex structures in the *Pcnt* mutant. (A) Expression of Pax6 (green) and Tbr1 (red), and Nestin in coronal sections of the E14.5 cerebral cortex. Scale bar: 50 μm. (B) Nissl-stained sagittal sections of the E18.5 cerebral cortex. Scale bar: 100 μm. (C) BrdU labeling assay. Cells were labeled with BrdU at E14.5, and analyzed at E17.5. Cells that incorporated BrdU were detected by anti-BrdU antibody. (D) Quantification of the distribution of BrdU-labeled cells along the radial axis of the control and mutant cortex at E17.5 after 3 days of BrdU injection (C). Mean and SEM are indicated. $Pcnt^{+/}$; n = 4 different animals, 2678 cells counted in total, $Pcnt^{-/-}$; n = 4 different animals, 2411 cells counted in total. *: $P < 0.05$ (Wilcoxon test). Scale bar: 100 μm. (E) Increased apoptosis and DNA double-strand breaks in the Pcnt mutant. E14.5 $Pcnt^{+/}$ and $Pcnt^{-/-}$ coronal brain sections were stained for Ki67, βIII-tubulin, Phospho-histone H3 (PH3), cleaved caspase-3, and γ-H2A.X. Scale bar: 50 μm (F) Quantification of cleaved caspase-3 or γ-H2A.X positive cells in the cerebral cortex. Bars indicate the mean values, and error bars represent SEM. $Pcnt^{+/}$ (n = 3 different animals), $Pcnt^{-/-}$ (n = 3 different animals), **: $P < 0.005$, ***: $P < 0.0001$ (t-test).

Studies Hybridoma Bank developed under the auspices of the NICHD and maintained by The University of Iowa, Department of Biological Sciences, Iowa City, IA 52242. This work was initiated at the Ernest Gallo Clinic and Research Center at the University of California, San Francisco, where support was provided by grants from the National Institutes of Health to A.S.P. It was also supported by postdoctoral fellowship from the Uehara Memorial Foundation to S.E-Y. and NARSAD Young Investigator Award to K.M.K. We thank the Gallo center for use of line 239 mice, and Y. Yanagawa and Gunma University for the transgenic GAD67-GFP line.

Appendix A. Supplementary data

Supplementary data associated with this article can be found, in the online version, at doi:10.1016/j.ydbio.2010.01.017.

References

Anitha, A., Nakamura, K., Yamada, K., Iwayama, Y., Toyota, T., Takei, N., Iwata, Y., Suzuki, K., Sekine, Y., Matsuzaki, H., Kawai, M., Miyoshi, K., Katayama, T., Matsuzaki, S., Baba, K., Honda, A., Hattori, T., Shimizu, S., Kumamoto, N., Tohyama, M., Yoshikawa, T., Mori, N., 2008. Gene and expression analyses reveal enhanced expression of pericentrin 2 (PCNT2) in bipolar disorder. Biol. Psychiatry 63, 678–685.

Anitha, A., Nakamura, K., Yamada, K., Iwayama, Y., Toyota, T., Takei, N., Iwata, Y., Suzuki, K., Sekine, Y., Matsuzaki, H., Kawai, M., Thanseem, I., Miyoshi, K., Katayama, T., Matsuzaki, S., Baba, K., Honda, A., Hattori, T., Shimizu, S., Kumamoto, N., Kikuchi, M., Tohyama, M., Yoshikawa, T., Mori, N., 2009. Association studies and gene expression analyses of the DISC1-interacting molecules, pericentrin 2 (PCNT2) and DISC1-binding zinc finger protein (DBZ), with schizophrenia and with bipolar disorder. Am. J. Med. Genet. B Neuropsychiatr. Genet. 150B, 967–976.

Anton, E.S., Ghashghaei, H.T., Weber, J.L., McCann, C., Fischer, T.M., Cheung, I.D., Gassmann, M., Messing, A., Klein, R., Schwab, M.H., Lloyd, K.C., Lai, C., 2004. Receptor tyrosine kinase ErbB4 modulates neuroblast migration and placement in the adult forebrain. Nat. Neurosci. 7, 1319–1328.

Ayala, R., Shu, T., Tsai, L.H., 2007. Trekking across the brain: the journey of neuronal migration. Cell 128, 29–43.

Badano, J.L., Teslovich, T.M., Katsanis, N., 2005. The centrosome in human genetic disease. Nat. Rev. Genet. 6, 194–205.

Baron, M., 2002. Manic-depression genes and the new millennium: poised for discovery. Mol. Psychiatry 7, 342–358.

Bellion, A., Baudoin, J.P., Alvarez, C., Bornens, M., Métin, C., 2005. Nucleokinesis in tangentially migrating neurons comprises two alternating phases: forward migration of the Golgi/centrosome associated with centrosome splitting and myosin contraction at the rear. J. Neurosci. 25, 5691–5699.

Capovilla, G., Lorenzetti, M.E., Montagnini, A., Borgatti, R., Piccinelli, P., Giordano, L., Accorsi, P., Caudana, R., 2001. Seckel's syndrome and malformations of cortical development: report of three new cases and review of the literature. J. Child Neurol. 16, 382–386.

Carfagnini, F., Tani, G., Ambrosetto, P., 1999. MR findings in Seckel's syndrome: report of a case. Pediatr. Radiol. 29, 849–850.

Caubit, X., Tiveron, M.C., Cremer, H., Fasano, L., 2005. Expression patterns of the three Teashirt-related genes define specific boundaries in the developing and postnatal mouse forebrain. J. Comp. Neurol. 486, 76–88.

Chen, D., Purohit, A., Halilovic, E., Doxsey, S.J., Newton, A.C., 2004. Centrosomal anchoring of protein kinase C betaII by pericentrin controls microtubule organization, spindle function, and cytokinesis. J. Biol. Chem. 279, 4829–4839.

Delaval, B., Doxsey, S.J., 2010. Pericentrin in cellular function and disease. J. Cell Biol. 188, 181–190.

Dictenberg, J.B., Zimmerman, W., Sparks, C.A., Young, A., Vidair, C., Zheng, Y., Carrington, W., Fay, F.S., Doxsey, S.J., 1998. Pericentrin and gamma-tubulin form a protein complex and are organized into a novel lattice at the centrosome. J. Cell Biol. 141, 163–174.

Diviani, D., Langeberg, L.K., Doxsey, S.J., Scott, J.D., 2000. Pericentrin anchors protein kinase A at the centrosome through a newly identified RII-binding domain. Curr. Biol. 10, 417–420.

Doxsey, S.J., Stein, P., Evans, L., Calarco, P.D., Kirschner, M., 1994. Pericentrin, a highly conserved centrosome protein involved in microtubule organization. Cell 76, 639–650.

Flames, N., Pla, R., Gelman, D.M., Rubenstein, J.L., Puelles, L., Marín, O., 2007. Delineation of multiple subpallial progenitor domains by the combinatorial expression of transcriptional codes. J. Neurosci. 27, 9682–9695.

Flory, M.R., Davis, T.N., 2003. The centrosomal proteins pericentrin and kendrin are encoded by alternatively spliced products of one gene. Genomics 82, 401–405.

Gillingham, A.K., Munro, S., 2000. The PACT domain, a conserved centrosomal targeting motif in the coiled-coil proteins AKAP450 and pericentrin. EMBO Rep. 1, 524–529.

Götz, M., Stoykova, A., Gruss, P., 1998. Pax6 controls radial glia differentiation in the cerebral cortex. Neuron 21, 1031–1044.

Gray, D.C., Hoeflich, K.P., Peng, L., Gu, Z., Gogineni, A., Murray, L.J., Eby, M., Kljavin, N., Seshagiri, S., Cole, M.J., Davis, D.P., 2007. pHUSH: a single vector system for conditional gene expression. BMC Biotechnol. 7, 61.

Griffith, E., Walker, S., Martin, C.A., Vagnarelli, P., Stiff, T., Vernay, B., Al Sanna, N., Saggar, A., Hamel, B., Earnshaw, W.C., Jeggo, P.A., Jackson, A.P., O'Driscoll, M., 2008. Mutations in pericentrin cause Seckel syndrome with defective ATR-dependent DNA damage signaling. Nat. Genet. 40, 232–236.

Gurling, H.M., Critchley, H., Datta, S.R., McQuillin, A., Blaveri, E., Thirumalai, S., Pimm, J., Krasucki, R., Kalsi, G., Quested, D., Lawrence, J., Bass, N., Choudhury, K., Puri, V., O'Daly, O., Curtis, D., Blackwood, D., Muir, W., Malhotra, A.K., Buchanan, R.W., Good, C.D., Frackowiak, R.S., Dolan, R.J., 2006. Genetic association and brain morphology studies and the chromosome 8p22 pericentriolar material 1 (PCM1) gene in susceptibility to schizophrenia. Arch. Gen. Psychiatry 63, 844–854.

Hand, R., Bortone, D., Mattar, P., Nguyen, L., Heng, J.I., Guerrier, S., Boutt, E., Peters, E., Barnes, A.P., Parras, C., Schuurmans, C., Guillemot, F., Polleux, F., 2005. Phosphorylation of Neurogenin2 specifies the migration properties and the dendritic morphology of pyramidal neurons in the neocortex. Neuron 48, 45–62.

Hevner, R.F., Shi, L., Justice, N., Hsueh, Y., Sheng, M., Smiga, S., Bulfone, A., Goffinet, A.M., Campagnoni, A.T., Rubenstein, J.L., 2001. Tbr1 regulates differentiation of the preplate and layer 6. Neuron 29, 353–366.

Higginbotham, H.R., Gleeson, J.G., 2007. The centrosome in neuronal development. Trends Neurosci. 30, 276–283.

Higginbotham, H., Tanaka, T., Brinkman, B.C., Gleeson, J.G., 2006. GSK3beta and PKCzeta function in centrosome localization and process stabilization during Slit-mediated neuronal repolarization. Mol. Cell. Neurosci. 32, 118–132.

Jaaro-Peled, H., Hayashi-Takagi, A., Seshadri, S., Kamiya, A., Brandon, N.J., Sawa, A., 2009. Neurodevelopmental mechanisms of schizophrenia: understanding disturbed postnatal brain maturation through neuregulin-1-ErbB4 and DISC1. Trends Neurosci. 32, 485–495.

Jurczyk, A., Gromley, A., Redick, S., San Agustin, J., Witman, G., Pazour, G.J., Peters, D.J., Doxsey, S., 2004. Pericentrin forms a complex with intraflagellar transport proteins and polycystin-2 and is required for primary cilia assembly. J. Cell Biol. 166, 637–643.

Kumar, R., Rawal, M., Agarwal, S., Gathwala, G., 2008. Semilobar holoprosencephaly in Seckel syndrome. Indian J. Pediatr. 75, 519–520.

Lewis, D.A., Pierri, J.N., Volk, D.W., Melchitzky, D.S., Woo, T.U., 1999. Altered GABA neurotransmission and prefrontal cortical dysfunction in schizophrenia. Biol. Psychiatry 46, 616–626.

Li, Q., Hansen, D., Killilea, A., Joshi, H.C., Palazzo, R.E., Balczon, R., 2001. Kendrin/pericentrin-B, a centrosome protein with homology to pericentrin that complexes with PCM-1. J. Cell Sci. 114, 797–809.

Liodis, P., Denaxa, M., Grigoriou, M., Akufo-Addo, C., Yanagawa, Y., Pachnis, V., 2007. Lhx6 activity is required for the normal migration and specification of cortical interneuron subtypes. J. Neurosci. 27, 3078–3089.

Lois, C., Alvarez-Buylla, A., 1994. Long-distance neuronal migration in the adult mammalian brain. Science 264, 1145–1148.

Long, J.E., Garel, S., Alvarez-Dolado, M., Yoshikawa, K., Osumi, N., Alvarez-Buylla, A., Rubenstein, J.L., 2007. Dlx-dependent and -independent regulation of olfactory bulb interneuron differentiation. J. Neurosci. 27, 3230–3243.

Majewski, F., Goecke, T., 1982. Studies of microcephalic primordial dwarfism I: approach to a delineation of the Seckel syndrome. Am. J. Med. Genet. 12, 7–21.

Majewski, F., Goecke, T.O., 1998. Microcephalic osteodysplastic primordial dwarfism type II: report of three cases and review. Am. J. Med. Genet. 80, 25–31.

Mao, Y., Ge, X., Frank, C.L., Madison, J.M., Koehler, A.N., Doud, M.K., Tassa, C., Berry, E.M., Soda, T., Singh, K.K., Biechele, T., Petryshen, T.L., Moon, R.T., Haggarty, S.J., Tsai, L.-H., 2009. Disrupted in schizophrenia 1 regulates neuronal progenitor proliferation via modulation of GSK3beta/beta-catenin signaling. Cell 136, 1017–1031.

Marín, O., Rubenstein, J.L., 2003. Cell migration in the forebrain. Annu. Rev. Neurosci. 26, 441–483.

Martinez-Campos, M., Basto, R., Baker, J., Kernan, M., Raff, J.W., 2004. The Drosophila pericentrin-like protein is essential for cilia/flagella function, but appears to be dispensable for mitosis. J. Cell Biol. 165, 673–683.

Matsuzaki, S., Tohyama, M., 2007. Molecular mechanism of schizophrenia with reference to disrupted-in-schizophrenia 1 (DISC1). Neurochem. Int. 51, 165–172.

Métin, C., Baudoin, J.P., Rakić, S., Parnavelas, J.G., 2006. Cell and molecular mechanisms involved in the migration of cortical interneurons. Eur. J. Neurosci. 23, 894–900.

Miyoshi, K., Asanuma, M., Miyazaki, I., Diaz-Corrales, F.J., Katayama, T., Tohyama, M., Ogawa, N., 2004. DISC1 localizes to the centrosome by binding to kendrin. Biochem. Biophys. Res. Commun. 317, 1195–1199.

Miyoshi, K., Asanuma, M., Miyazaki, I., Matsuzaki, S., Tohyama, M., Ogawa, N., 2006. Characterization of pericentrin isoforms in vivo. Biochem. Biophys. Res. Commun. 351, 745–749.

Miyoshi, K., Kasahara, K., Miyazaki, I., Shimizu, S., Taniguchi, M., Matsuzaki, S., Tohyama, M., Asanuma, M., 2009. Pericentrin, a centrosomal protein related to microcephalic primordial dwarfism, is required for olfactory cilia assembly in mice. FASEB J. 23, 3289–3297.

Numata, S., Iga, J., Nakataki, M., Tayoshi, S., Tanahashi, T., Itakura, M., Ueno, S., Ohmori, T., 2009a. Positive association of the pericentrin (PCNT) gene with major depressive disorder in the Japanese population. J. Psychiatry Neurosci. 34, 195–198.

Numata, S., Nakataki, M., Iga, J.I., Tanahashi, T., Nakadoi, Y., Ohi, K., Hashimoto, R., Takeda, M., Itakura, M., Ueno, S.I., Ohmori, T., 2009b. Association study between the pericentrin (PCNT) gene and schizophrenia. Neuromolecular. Med.

Piane, M., Della Monica, M., Piatelli, G., Lulli, P., Lonardo, F., Chessa, L., Scarano, G., 2009. Majewski osteodysplastic primordial dwarfism type II (MOPD II) syndrome previously diagnosed as Seckel syndrome: report of a novel mutation of the PCNT gene. Am. J. Med. Genet. A 149A, 2452–2456.

Polleux, F., Ghosh, A., 2002. The slice overlay assay: a versatile tool to study the influence of extracellular signals on neuronal development. Sci. STKE PL9.

Rauch, A., Thiel, C.T., Schindler, D., Wick, U., Crow, Y.J., Ekici, A.B., van Essen, A.J., Goecke, T.O., Al-Gazali, L., Chrzanowska, K.H., Zweier, C., Brunner, H.G., Becker, K., Curry, C.J., Dallapiccola, B., Devriendt, K., Dörfler, A., Kinning, E., Megarbane, A., Meinecke, P.,

Semple, R.K., Spranger, S., Toutain, A., Trembath, R.C., Voß, E., Wilson, L., Hennekam, R., de Zegher, F., Dörr, H.G., Reis, A., 2008. Mutations in the pericentrin (PCNT) gene cause primordial dwarfism. Science 319, 816–819.
Shanske, A., Caride, D.G., Menasse-Palmer, L., Bogdanow, A., Marion, R.W., 1997. Central nervous system anomalies in Seckel syndrome: report of a new family and review of the literature. Am. J. Med. Genet. 70, 155–158.
Solecki, D.J., Model, L., Gaetz, J., Kapoor, T.M., Hatten, M.E., 2004. Par6alpha signaling controls glial-guided neuronal migration. Nat. Neurosci. 7, 1195–1203.
Stenman, J., Toresson, H., Campbell, K., 2003. Identification of two distinct progenitor populations in the lateral ganglionic eminence: implications for striatal and olfactory bulb neurogenesis. J. Neurosci. 23, 167–174.
Stühmer, T., Anderson, S.A., Ekker, M., Rubenstein, J.L., 2002. Ectopic expression of the Dlx genes induces glutamic acid decarboxylase and Dlx expression. Development 129, 245–252.
Takahashi, M., Yamagiwa, A., Nishimura, T., Mukai, H., Ono, Y., 2002. Centrosomal proteins CG-NAP and kendrin provide microtubule nucleation sites by anchoring gamma-tubulin ring complex. Mol. Biol. Cell 13, 3235–3245.
Tamamaki, N., Yanagawa, Y., Tomioka, R., Miyazaki, J., Obata, K., Kaneko, T., 2003. Green fluorescent protein expression and colocalization with calretinin, parvalbumin, and somatostatin in the GAD67-GFP knock-in mouse. J. Comp. Neurol. 467, 60–79.
Tsai, L.H., Gleeson, J.G., 2005. Nucleokinesis in neuronal migration. Neuron 46, 383–388.
Turetsky, B.I., Moberg, P.J., Yousem, D.M., Doty, R.L., Arnold, S.E., Gur, R.E., 2000. Reduced olfactory bulb volume in patients with schizophrenia. Am. J. Psychiatr. 157, 828–830.
Willems, M., Genevieve, D., Borck, G., Baumann, C., Baujat, G., Bieth, E., Edery, P., Farra, C., Gerard, M., Heron, D., Leheup, B., Le Merrer, M., Lyonnet, S., Martin-Coignard, D., Mathieu, M., Thauvin-Robinet, C., Verloes, A., Colleaux, L., Munnich, A., Cormier-Daire, V., 2009. Molecular analysis of pericentrin gene (PCNT) in a series of 24 Seckel/ MOPD II families. J. Med. Genet. (Epub 2009 Nov 4).
Wonders, C.P., Anderson, S.A., 2006. The origin and specification of cortical interneurons. Nat. Rev. Neurosci. 7, 687–696.
Xu, Q., Cobos, I., De La Cruz, E., Rubenstein, J.L., Anderson, S.A., 2004. Origins of cortical interneuron subtypes. J. Neurosci. 24, 2612–2622.
Zarbalis, K., May, S.R., Shen, Y., Ekker, M., Rubenstein, J.L., Peterson, A.S., 2004. A focused and efficient genetic screening strategy in the mouse: identification of mutations that disrupt cortical development. PLoS Biol. 2, E219.
Zhao, Y., Flandin, P., Long, J.E., Cuesta, M.D., Westphal, H., Rubenstein, J.L., 2008. Distinct molecular pathways for development of telencephalic interneuron subtypes revealed through analysis of Lhx6 mutants. J. Comp. Neurol. 510, 79–99.
Zimmerman, W.C., Sillibourne, J., Rosa, J., Doxsey, S.J., 2004. Mitosis-specific anchoring of gamma tubulin complexes by pericentrin controls spindle organization and mitotic entry. Mol. Biol. Cell 15, 3642–3657.